On the RFI Detection in Differential Interferometric Synthetic Aperture Radar

Yanyang Liu[1], Mingliang Tao[2], Jieshuang Li[2], Tao Li[3], Junli Chen[4]

[1] Shanghai Institute of satellite engineering, Shanghai 201109, China
[2] School of Electronics and Information, Northwestern Polytechnical University, 710072 Xi'an, China
[3] Land Satellite Remote Sensing Application Center, Ministry of Natural Resources of P.R. China, Beijing, 100048, China
[4] Shanghai Academy of Spaceflight Technology, Shanghai 201109, China

Keywords: Synthetic aperture radar (SAR), Differential interferometric SAR (D-InSAR), Radio frequency interference (RFI), RFI detection, Clutter suppression.

Abstract

Synthetic Aperture Radar (SAR) can image the ground with a wide area and high resolution at all times and in all weather and has become an important means of remote sensing. Differential interferometry SAR technology can obtain high-precision surface deformation information by processing more than two SAR images before and after deformation. In recent years, it has attracted widespread attention and research. However, due to the increasing number of ground electronic devices, ground radio frequency interference (RFI) has become one of the main problems in differential interferometry SAR processing, seriously affecting the performance of differential interferometry SAR imaging and differential interferometry surface deformation monitoring applications. In this paper, a clutter cancellation interference enhancement detection algorithm is proposed. By clutter suppression in the primary and secondary images, the interference-to-signal ratio is increased, which effectively improves the interference detection capabilities. The effectiveness of the algorithm in this paper is verified by the on-orbit measured data of the Lutan-1 satellites.

1. Introduction

Spectrum allocation is a crucial foundation for determining the operational frequency band of satellites, which significantly impacts the detection efficiency of remote sensing (Chen J., et al., 2024). However, the limited spectrum available for active remote sensing is also extensively shared with other radio services. Consequently, Synthetic Aperture Radar (SAR) cannot evade the threat posed by other radio radiation sources and inevitably receives echoes of signals transmitted from various electromagnetic devices. This phenomenon is referred to as Radio Frequency Interference (RFI) (Moreira A. 2013, Tao M., 2019).

RFI presents a significant challenge in the context of limited spectral resources, as it conflicts with the desired echo signal and leads to distortion and interpretation difficulties in remote sensing data. RFI can directly perturb the amplitude and phase of the image, resulting in masking artifacts with distinctive texture patterns or even complete occlusion of the target scene (Tao M., et al, 2019, Huang Y., et al.,2022). This obscures the spatial and radiation response information of actual targets, severely undermining the reliability of qualitative interpretation applications such as land classification, coherent change detection, and target recognition (Tao M., et al, 2019). In particular, for Differential Interferometry Synthetic Aperture Radar (D-InSAR) technology, the amplitude and phase distortion errors caused by RFI can have a profound impact on various aspects of the process (Xu H., et al., 2015). These include registration, polarization correlation, interferometric phase maps, and more, ultimately leading to errors in deformation detection (Chen J., et al., 2024). To mitigate these effects, it is essential to develop robust algorithms and techniques that can effectively identify and suppress RFI, thereby enhancing the quality and reliability of remote sensing data and its applications.

LuTan-1 (LT-1), China's first L-band differential interferometry synthetic aperture radar satellite, primarily focuses on land monitoring (Li T., et al. 2022). Launched in February 2022, it provides high-precision surface deformation monitoring, topographic mapping, and other essential tasks within the designated area through a twin satellite constellation. Operating at the L-band with a center frequency of 1.26 GHz and a maximum signal bandwidth of 80 MHz, LuTan-1 is well-suited for land monitoring applications due to its exceptional penetration capability. This allows for accurate retrieval of surface scattering characteristics and deformation parameters. However, the L-band InSAR system's relatively large receiving bandwidth and beamwidth, coupled with shared spectrum usage with various radio services, lead to radio frequency interference (RFI) that poses a significant challenge to the SAR data recording, processing, and interpretation phases. Therefore, it is crucial to develop processing pipeline to minimize the adverse effects of RFI and ensure the satellite's core missions of land monitoring and deformation analysis effectively (Chen J., et al., 2024).

A significant amount of research has been conducted to mitigate RFI artifacts from the standpoint of signal processing (Tao M., et al, 2019, Liu Y., et al., 2023). Tao et al. offer a comprehensive overview of relevant signal processing techniques. Among the most prevalent methods is adaptive filtering, which devises optimal filters within the time, frequency, or time-frequency domain (Meyer F. J., 2013. Natsuaki R., 2017. Natsuaki R., 2022). Although this approach is straightforward and effective, it tends to distort the target signals when confronting intricate RFI. Numerous researchers have put forth sophisticated interference separation and signal reconstruction methodologies, including the low-rank and sparse decomposition model (Huang Y., et al.,2021), as well as alternating projection techniques (Lv Z., et al., 2024). Nonetheless, these methods may not adequately recover the phase, which poses challenges for interferometric applications.

The LuTan-1 processor currently employs a two-stage method for RFI detection and mitigation based on a single SAR data, leading to a significant improvement in image quality (Chen J., et al., 2024). In the first stage, the Signal Protection Module applies window removal to the signal and performs a Fourier transform on its range dimension to obtain the range-frequency domain. The natural logarithm of the observed data is used as a test statistic, which follows a Gaussian distribution. To address strong signals disrupting the azimuth direction's Gaussian

distribution characteristics, a Z statistical hypothesis test is conducted on a sliding window along the range direction to determine the positions of strong signals. A confidence level is established, and a frequency matrix is calculated to obtain a protective mask through histogram statistics and binarization processing. In the second stage, the remaining observed data with strong signals removed is utilized for interference detection. The logarithmic modulus of each pulse still follows a Gaussian distribution, with RFI distributed along the azimuth direction. The Z test is performed on a sliding window along the azimuth direction to determine the position of RFI, considering the number of range sampling points. This two-stage approach effectively identifies and mitigates RFI artifacts while maintaining the integrity of the target signals.

It is important to note that the performance of this two-stage method is dependent on the interference-to-signal ratio (ISR) (Chen J., et al., 2024). In the context of D-InSAR processing, the ISR can be enhanced by utilizing two D-InSAR SAR images. This allows for the detection of weaker RFI signals that might otherwise go unnoticed. In this paper, we propose a novel approach for detecting and mitigating RFI in D-InSAR systems. The organization of the paper is as follows: Section 2 provides a brief overview of the different types of RFI and their impact on D-InSAR operations. This section highlights the challenges posed by RFI and the need for effective detection and mitigation strategies. Section 3 details the current RFI detection method employed by the LuTan-1 (LT-1) satellite and introduces the proposed algorithm. This section describes the key principles, features, and advantages of the proposed approach, emphasizing its potential for improving D-InSAR performance in the presence of RFI. Section 4 presents experimental results obtained from LuTan-1 D-InSAR data to validate the effectiveness of the proposed method. These results demonstrate the ability of the proposed approach to accurately detect and mitigate RFI, leading to improved data quality and reliability. Finally, Section 5 concludes the paper, summarizing the main findings and contributions of the research, and discussing future directions for further development and application of the proposed RFI detection and mitigation technique.

2. The effect of RFI on D-InSAR

Based on the relative bandwidth, Radio Frequency Interference (RFI) signals can be categorized into two types: Time Stationary Narrow Band (TSNB) Interference and Time-Varying Wide Band (TVWB) Interference (Tao M., et al, 2019). Amateur radio services are a common source of TSNB, while ground-based radiolocation radars, such as ASAR-4, intermittently emit pulse signals that can lead to intermittent wideband RFI in Synthetic Aperture Radar (SAR) sensors, referred to as TVWB. Figure 1 illustrates the temporal relationships of the two types of interference in both the range-time domain and the range-frequency domain. This visualization demonstrates the mechanisms of TSNB and TVWB through a time diagram, providing insights into their distinct characteristics and behaviours in the context of SAR systems. Understanding these interference types is crucial for developing effective detection and mitigation strategies to enhance the quality and reliability of remote sensing data (Chen J., et al., 2024).
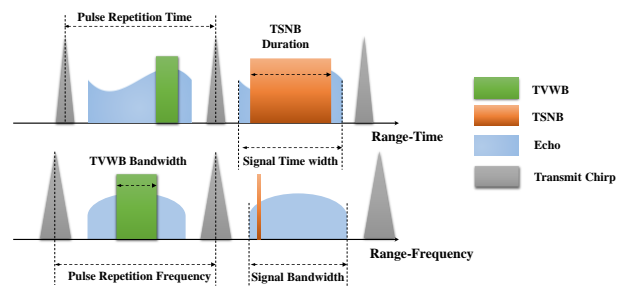

Figure. 1 . Illustration of the mechanism of TSNB and TVWB in the form of a time and frequency diagram (Chen J., et al., 2024).
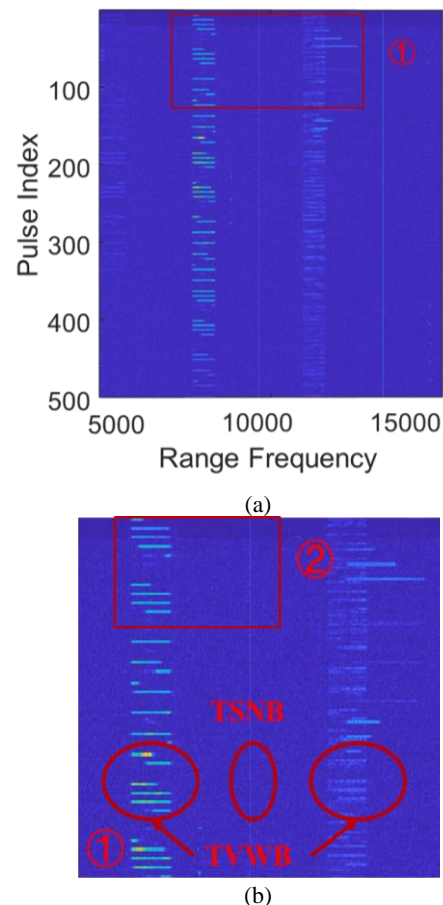

(a)

(b)

Figure. 2 A particular example of an RFI-affected LuTan-1 frame. (a) Range Spectrum of the echo data. (b) The enlarged ROI of the range spectrum of the echo data (Chen J., et al., 2024).

Figure 2 showcases a specific RFI case recorded by the LuTan-1 (LT-1) system in Inner Mongolia, China (Chen J., et al., 2024). The range spectrum of the data is presented in Figure 2(a), where the bands with intermittently stronger energy relative to the target echo indicate TVWB. Red ellipses highlight partially occurring RFI in Figure 2(b), where the bright thin line along the azimuth represents TSNB.

Since the imaging process is linear, then with the presence of RFI, the SAR SLC image H_i can be written as

$$H_i = S_i + I_i + N_i \qquad (1)$$

where S_i, I_i and N_i represent the useful signal, interference, and system noise, respectively.

The coherence between pixel pairs of two SAR images is estimated as (Touzi R., et al., 1999)

$$\gamma = \frac{\mathrm{E}\{H_1 H_2^*\}}{\sqrt{\mathrm{E}\{|H_1|^2\}\mathrm{E}\{|H_2|^2\}}} \qquad (2)$$

Assuming that S_i, I_i and N_i are independent of others, N_1 and N_2 are also independent, then

$$\gamma = \frac{\mathrm{E}\{S_1 S_2^*\} + \mathrm{E}\{I_1 I_2^*\}}{\sqrt{\mathrm{E}\{|S_1|^2 + |I_1|^2 + |N_1|^2\}\mathrm{E}\{|S_2|^2 + |I_2|^2 + |N_2|^2\}}} \qquad (3)$$

Here, we define

$$\mathrm{E}\{S_1 S_2^*\} = \gamma_S \sigma_{S,1}\sigma_{S,2}\exp(j\varphi_{S,1,2}) \qquad (4)$$

$$\mathrm{E}\{I_1 I_2^*\} = \gamma_I \sigma_{I,1}\sigma_{I,2}\exp(j\varphi_{I,1,2}) \qquad (5)$$

where $\varphi_{S,1,2}$ is the phase difference between S_1 and S_2, $\varphi_{I,1,2}$ is the phase difference between I_1 and I_2, and σ_{S1}, σ_{S2}, σ_{I1} and σ_{I2} denote the variance of S_1, S_2, I_1 and I_2, respectively. It is worth noting that σ_{S1}^2, σ_{S2}^2, σ_{I1}^2 and σ_{I2}^2 represents the energy of S_1, S_2, I_1 and I_2.

The pixel pair coherence can be further rewritten as follows (Chen J., et al., 2024):

$$\gamma = \frac{\sigma_{S1}\cdot\sigma_{S2}\cdot\gamma_S\exp(j\varphi_{S,1,2}) + \sigma_{I1}\cdot\sigma_{I2}\cdot\gamma_I\exp(j\varphi_{I,1,2})}{\sqrt{\sigma_{S1}^2+\sigma_{I1}^2+\sigma_{N1}^2}\sqrt{\sigma_{S2}^2+\sigma_{I2}^2+\sigma_{N2}^2}} \qquad (6)$$

From the aforementioned equation, it becomes evident that jamming not only degrades the coherence but also impacts the interferometric phase when the jamming present in two images exhibits coherence. To illustrate these effects, Figure 3 displays an example scenario comparing an LT-1 acquisition with RFI and another without RFI. As observed in the figure, most regions free from interference appear white, signifying a high coherence coefficient close to 1. In contrast, areas affected by RFI exhibit low coherence. Consequently, it is essential to remove the jamming prior to D-InSAR processing to ensure accurate and reliable results. This step is crucial for maintaining the integrity of remote sensing data and enhancing the performance of applications such as land classification, coherent change detection, and target recognition.
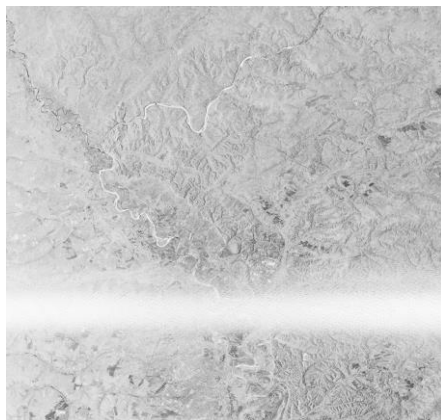
(a)

(b)
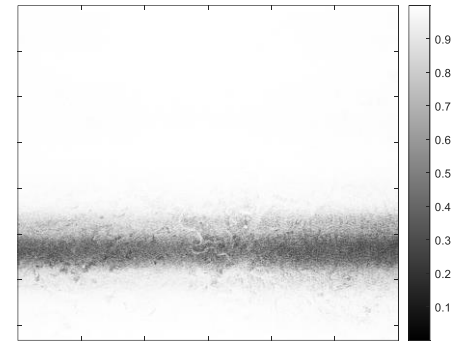
(c)

Figure. 1 Repeat-pass SAR images with RFI. (a) Master SAR image with RFI. (b) Slave SAR image without RFI. (c) Coherence between master and slave SAR images.

3. RFI Detection and Mitigation in D-InSAR

To enhance the performance of Radio Frequency Interference (RFI) detection, clutter suppression techniques are employed in this approach to improve the interference-to-signal ratio (ISR). Clutter suppression aims to minimize the impact of unwanted signals, such as background noise and environmental disturbances, on the quality of the received data. By applying clutter suppression algorithms, the ISR can be increased, making it easier to detect and mitigate RFI. This is particularly beneficial in scenarios where the RFI signals are weak or masked by strong background clutter. The fundamental principle underlying this strategy is as follows:

$$\begin{aligned}\Delta H &= H_1 - H_2 \exp(j\varphi_{S,1,2}) \\ &= \Delta S + \Delta I + \Delta N\end{aligned} \qquad (7)$$

where $\Delta S = S_1 - S_2 \exp(j\varphi_{S,1,2})$,

$\Delta I = I_1 - I_2 \exp(j\varphi_{S,1,2})$,

$\Delta N = N_1 - N_2 \exp(j\varphi_{S,1,2})$.

The expected energy of residual signals can be expressed as

$$\sigma_{\Delta S}^2 = \mathrm{E}\left\{\left|S_1 - S_2 \exp(j\varphi_{S,1,2})\right|^2\right\} \qquad (8)$$

Supposing the two images are well radiometric calibration, it can be considered that $\sigma_{S1}{}^2 = \sigma_{S2}{}^2 = \sigma_s{}^2$, and (11) can be further expressed as follows

$$\sigma_{\Delta S}^2 = E\left\{|S_1|^2\right\} + E\left\{|S_2|^2\right\} - E\left\{S_1 S_2^* \exp\left(-j\varphi_{S,1,2}\right)\right\} - E\left\{S_2 S_1^* \exp\left(j\varphi_{S,1,2}\right)\right\}$$
$$= 2\sigma_s^2\left(1-|\gamma|\right) \tag{9}$$

When $\gamma > 0.5$, the energy of residual signals would be lower than σ_s^2. It can be deduced that if only one of these two images is polluted by RFI, the ISR of clutter-suppressed image can be improved, enabling more accurate and robust RFI detection and mitigation.
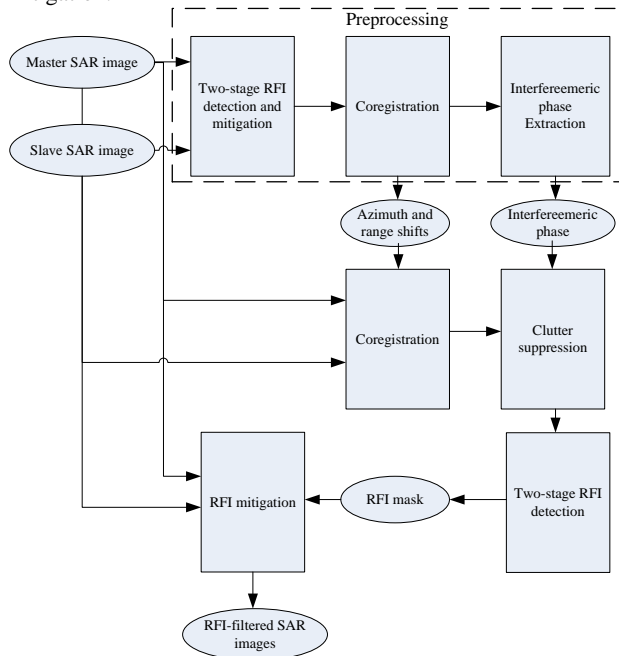

Figure. 4 Flowchart of the RFI detection and mitigation scheme proposed in this paper.

Building upon the principle outlined above, we propose a novel RFI detection method. The flowchart of the proposed method is illustrated in Figure 4, which consists of the following steps:

(1) Pre-processing
In this initial step, the azimuth and range shifts between the original Synthetic Aperture Radar (SAR) images, as well as the interferometric phase $\hat{\varphi}_{S,1,2}$, are estimated using the SAR images filtered by Chen's two-stage RFI detection and mitigation method (Chen J., et al., 2024). This step ensures that strong potential RFI is accounted for during the subsequent processing stages.

(2) Registration of the original SAR images
To address the issue that RFI can lead to suboptimal registration of the two original SAR images, the azimuth and range shifts obtained in step (1) are employed to align the images accurately. Proper registration is crucial for accurate RFI detection and mitigation, as well as for maintaining the overall quality of the interferometric data.

(3) Clutter suppression
To enhance the performance of RFI detection, clutter suppression techniques are applied to improve the interference-to-signal ratio (ISR). By reducing the impact of unwanted

signals, making it easier to detect and mitigate RFI. This step is particularly important in scenarios where the RFI signals are weak or masked by strong background clutter.

$$\Delta H = H_1 - H_2 \exp\left(j\hat{\varphi}_{S,1,2}\right) \tag{10}$$

where the interferometric phase $\hat{\varphi}_{S,1,2}$ is estimated in step (1).

(4) Two-stage RFI detection
The two-stage Radio Frequency Interference (RFI) detection method (Chen J., et al., 2024), is applied to the clutter-suppressed SAR images to generate an RFI mask $Mask_{final,1}(f,t)$.
This mask identifies the pixels contaminated by RFI, facilitating their subsequent mitigation.

(5) RFI mitigation
To mitigate the identified RFI, the RFI mask is utilized for notched filtering of the original SAR images. Notched filtering involves selectively removing the frequency components associated with RFI while preserving the rest of the signal. This results in the final RFI-mitigated SAR images, which are free from the adverse effects of RFI and ready for further analysis and applications in remote sensing.

By following these steps, the proposed RFI detection method can effectively identify and mitigate RFI in D-InSAR data, , ensuring the production of high-quality and reliable D-InSAR products for change detection.

4. Experimental results

This section presents the experimental results of the proposed Radio Frequency Interference (RFI) detection and mitigation method for example scenario applications. To provide a quantitative analysis of the method's RFI suppression performance, the average coherence coefficient of interferometric measurements is also calculated, as defined in equation (2).

Figures5(a) and 5(b) depict the range-frequency domain of the example polluted scenario before and after applying the proposed cancellation method, respectively. These figures illustrate that the weak RFI is more pronounced and easier to detect after employing the proposed cancellation technique. Figure 5(c) demonstrates that a significant amount of RFI has been successfully removed, resulting in an improved high-quality Synthetic Aperture Radar (SAR) image. Figure 6(d) displays the grayscale coherence coefficient map after RFI suppression, where white (with a value of 1) corresponds to the maximum coherence coefficient and black (with a value of 0) corresponds to the minimum. A comparison with Figure 3(c) reveals a substantial improvement in the correlation coefficient. Table I presents the results of the average correlation coefficient before and after RFI suppression. The mean coherence coefficient of the image after mitigation reaches a value of 0.9662, marking an increase of 0.0416 compared to the pre-mitigation state. These experimental results confirm the effectiveness of the proposed RFI detection and mitigation method in enhancing the quality and reliability of remote sensing data, particularly in the presence of RFI.
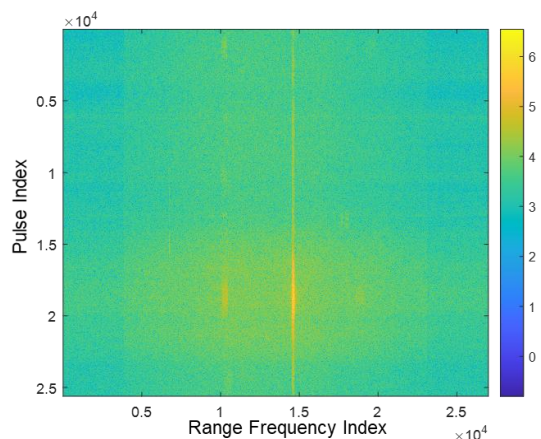
(a)

(b)

(c)

(d)
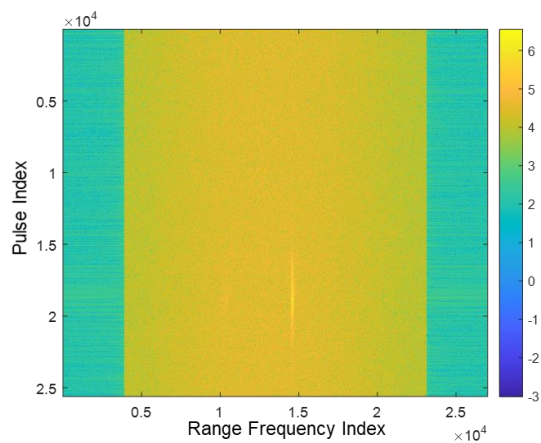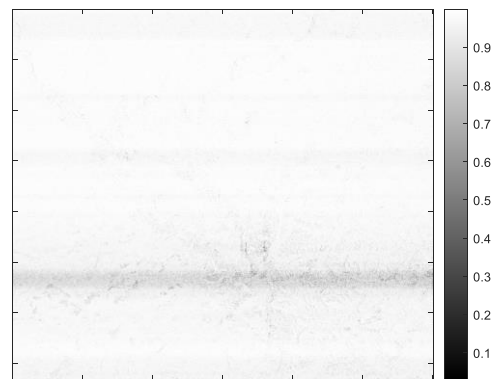
Figure. 5 Processed result of the example scenario. (a) the range-frequency domain before cancellation. (b) the range-frequency domain after cancellation. (c) Master SAR image after RFI suppression. (d) Coherence between master and slave SAR images after RFI suppression.

Parameter	Before	After
Average correlation coefficient	0.9246	0.9662

Table I Average correlation coefficient

5. Conclusion

In this paper, we have proposed a novel Radio Frequency Interference (RFI) detection and mitigation method for D-InSAR systems. The method utilizes clutter suppression techniques to improve the interference-to-signal ratio (ISR), enabling more accurate and robust RFI detection and mitigation. The experimental results demonstrate that the proposed method effectively identifies and removes RFI, leading to significant improvements in image quality and coherence. The method has been successfully applied to LuTan-1 (LT-1) D-InSAR data. The experimental results reveal that the coherence coefficient of the image after mitigation reaches a value of 0.9662, an increase of 0.0416 compared to before mitigation. The proposed RFI detection and mitigation method offers a valuable solution for addressing the challenges posed by RFI in D-InSAR systems.

References

Chen J., et al., *Characterization and Mitigation of Radio Frequency Interference Signatures in L-Band LuTan-1 InSAR System: First Results and Assessment*, IEEE Transactions on Radar Systems, vol. 2, pp. 404-420, 2024.

Huang Y., et al., *HRWS SAR narrowband interference mitigation using low-rank recovery and image-domain sparse regularization*. IEEE Transactions on Geoscience and Remote Sensing, vol. 60, pp. 1-14, 2021.

Huang Y. et al., *An Efficient Radio Frequency Interference Mitigation Algorithm in Real Synthetic Aperture Radar Data*. IEEE Transactions on Geoscience and Remote Sensing, vol. 60, pp. 1-12, 2022.

Li T., Tang X., Zhou X., and Zhang X., "LuTan-1 SAR Main Applications and Products," EUSAR 2022; 14th European Conference on Synthetic Aperture Radar, pp. 1-4. VDE, 2022.

Liu Y., et al., *RFI Detection for Multichannel HRWS SAR System Based on Spatial Cross Correlation.* Journal of Beijing Institute of technology, 2023, 32(6): 696-703.

Lv Z., et al., *A Two-Stage Approach for TSNB and ITWB RFI Mitigation in P- and L-Band SAR Data*, IEEE Transactions on Aerospace and Electronic Systems, vol. 60, no. 2, pp. 1450-1470, April 2024.

Meyer F. J., et al., *Correction and characterization of radio frequency interference signatures in L-band synthetic aperture radar data*, IEEE Transactions on Geoscience and Remote Sensing, vol. 51, no. 10, pp. 4961-4972, 2013.

Moreira A., Prats-Iraola,P. Younis M., Krieger G., Hajnsek I., and Papathanassiou K. P., "A tutorial on synthetic aperture radar," IEEE Geosci. Remote Sens. Mag., vol. 1, no. 1, pp. 6–43, Mar. 2013.

Natsuaki R., Motohka T., Suzuki S., and Tadono T., *Radio frequency interference in ALOS-2 PALSAR-2 interferogram*, 2017 XXXIInd General Assembly and Scientific Symposium of the International Union of Radio Science (URSI GASS), Montreal, QC: IEEE, Aug. 2017, pp. 1–4.

Natsuaki R. and Hirose A., *Polarimetric Analysis of RFI in L-Band SAR System*, 2022 IEEE International Geoscience and Remote Sensing Symposium (IGARSS 2022), Kuala Lumpur, Malaysia: IEEE, Jul. 2022, pp. 5145–5148.

Tao M., et al., *Mitigation of Radio Frequency Interference in Synthetic Aperture Radar Data: Current Status and Future Trends.* Remote Sens. 2019, 11, 2438.

Touzi R., Lopes A., Bruniquel J. and Vachon P. W., *Coherence estimation for SAR imagery*. IEEE Transactions on Geoscience and Remote Sensing, vol. 37, no. 1, pp. 135-149, Jan. 1999.

Xu H., et al., *Analysis of the Effect of Interference on InSAR*, IEEE Sensors Journal, vol. 15, no. 10, pp. 5659-5668, Oct. 2015.